JUSTC

Article

http://justc.ustc.edu.cn

Received: November 16, 2021; Accepted: January 18, 2022

Size-reduction of Rydberg collective excited states in cold atomic system

Dongsheng Ding[1,2,*] ✉, Yichen Yu[1,2,*], Zongkai Liu[1,2], Baosen Shi[1,2] ✉, and Guangcan Guo[1,2]

[1]*Key Laboratory of Quantum Information, University of Science and Technology of China, Hefei 230026, China;*
[2]*Synergetic Innovation Center of Quantum Information and Quantum Physics, University of Science and Technology of China, Hefei 230026, China*

* These authors contributed equally to this work
✉Correspondence: Dongsheng Ding, E-mail: dds@ustc.edu.cn; Baosen Shi, E-mail: drshi@ustc.edu.cn

Graphical abstract

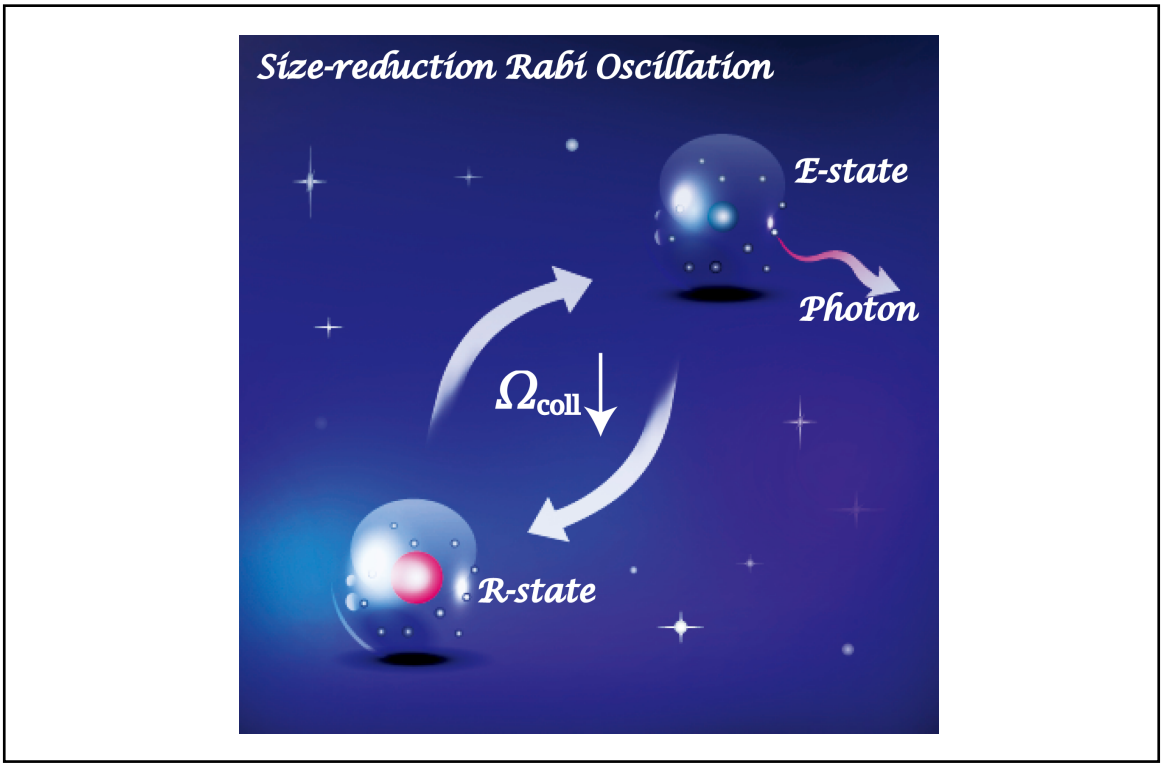

A size-reduction effect of the Rydberg collective state during Rabi oscillation. E-state: low-lying collective excited state. R-state: high-lying Rydberg collective excited state. Ω_{coll}: the effective Rabi frequency.

Public summary

- The Rydberg collective state is firstly created by Rydberg quantum memory, the authors demonstrate a decreased oscillation frequency effect via measuring time traces of the retrieved light field amplitude, exhibiting a chirped characteristic.
- This many-body Rabi oscillation between a high-lying Rydberg collective excited state and low-lying collective excited state is accompanying with a radiated photon.
- This experiment shows potential perspectives in manipulating single photon shape and controlling Rydberg superatoms.

Citation: Ding D S, Yu Y C, Liu Z K, et al. Size-reduction of Rydberg collective excited states in cold atomic system. *JUSTC*, **2022**, 52(4): 1. DOI: 10.52396/JUSTC-2021-0239

JUSTC

Article

http://justc.ustc.edu.cn

Received: November 16, 2021; Accepted: January 18, 2022

Size-reduction of Rydberg collective excited states in cold atomic system

Dongsheng Ding[1,2,*] ✉, Yichen Yu[1,2,*], Zongkai Liu[1,2], Baosen Shi[1,2] ✉, and Guangcan Guo[1,2]

[1]*Key Laboratory of Quantum Information, University of Science and Technology of China, Hefei 230026, China;*
[2]*Synergetic Innovation Center of Quantum Information and Quantum Physics, University of Science and Technology of China, Hefei 230026, China*

* These authors contributed equally to this work
✉Correspondence: Dongsheng Ding, E-mail: dds@ustc.edu.cn; Baosen Shi, E-mail: drshi@ustc.edu.cn

Cite This: *JUSTC*, **2022**, 52(4): 1 (6pp)

Read Online

Abstract: The collective effect of large amounts of atoms exhibit an enhanced interaction between light and atoms. This holds great interest in quantum optics, and quantum information. When a collective excited state of a group of atoms during Rabi oscillation is varying, the oscillation exhibits rich dynamics. Here, we experimentally observe a size-reduction effect of the Rydberg collective state during Rabi oscillation in cold atomic dilute gases. The Rydberg collective state was first created by the Rydberg quantum memory, and we observed a decreased oscillation frequency effect by measuring the time traces of the retrieved light field amplitude, which exhibited chirped characteristics. This is caused by the simultaneous decay to the overall ground state and the overall loss of atoms. The observed oscillations are dependent on the effective Rabi frequency and detuning of the coupling laser, and the dephasing from inhomogeneous broadening. The reported results show the potential prospects of studying the dynamics of the collective effect of a large amount of atoms and manipulating a single-photon wave-packet based on the interaction between light and Rydberg atoms.

Keywords: Rydberg atom; quantum storage; collective excited states

CLC number: O431.2 **Document code:** A

1 Introduction

The interaction of light with an atomic media containing a large number of particles causes a collective effect[1], which is at the focus of intense research in different areas in quantum metrology, quantum optics, and quantum information. The single collective excitation shared among a large number of ground-state atoms results in a coherent superposition state[2, 3]. In contrast to the single atom coupled to the light field this state can still carry only a single excitation; however, the light matter interaction is enhanced owing to a large number of ground state atoms, as predicted by Dicke's theory. When the single excitation corresponds to the Rydberg excitation, Rydberg-state super atoms were formed[4–11] consisting of a single Rydberg excitation and many ground state atoms. Because of the exaggerated properties of the Rydberg atom, it is a valuable resource for numerous potential applications in quantum computing[12, 13], quantum optics[14], and many-body physics[15–18] etc.

Storing photons to Rydberg super atoms can be realized by the technology of quantum memory[19, 20], in which an interface between light and Rydberg atoms is created that allows for the storage and retrieval of the optical field. Demonstrating a Rydberg-mediated quantum memory could enable the implementation of quantum computation and information processing with the advantages of Rydberg super atoms, for example, by converting a Rydberg super atom to a single photon, the demonstration of a deterministic single-photon generator can be realized[21, 22]. Coherently preparing and manipulating the Rydberg super atom based on quantum memory holds promise in quantum information science; it is deserved to be studied. When the stored collective excited state is driven by the read field, a Rabi oscillation dynamics of the quantum reading process as studied in a double-Λ system[23–25], however, an anomalous reduction-frequency oscillation with a varying frequency has never been reported before.

In this work, we prepared a Rydberg super atom through quantum memory in the Rydberg electromagnetically induced transparency (Rydberg EIT) configuration. Rabi oscillation between the low-lying collective excited-state and high-lying Rydberg-state super atom is realized by driving the coupling laser in the reading process. The retrieved probe pulse exhibits chirped characteristics because of the reduction of the effective size of the Rydberg super atom. Combining the two-level atoms dephasing model extracted from inhomogeneous broadening, we model our experimental observations with a decreased-frequency Rabi oscillation function. The coherent Rabi oscillation in the Rydberg quantum memory process is a new representation for combining the collective dynamical behavior of Rydberg atoms and the radiation of a single photon, which is crucial for the applications of Rydberg atoms in quantum information processing[26] and for providing a versatile interface between light and atoms.

2 Experimental setup

The schematics of the energy levels, experimental setup, and

DOI: 10.52396/JUSTC-2021-0239
JUSTC, **2022**, 52(4): 1

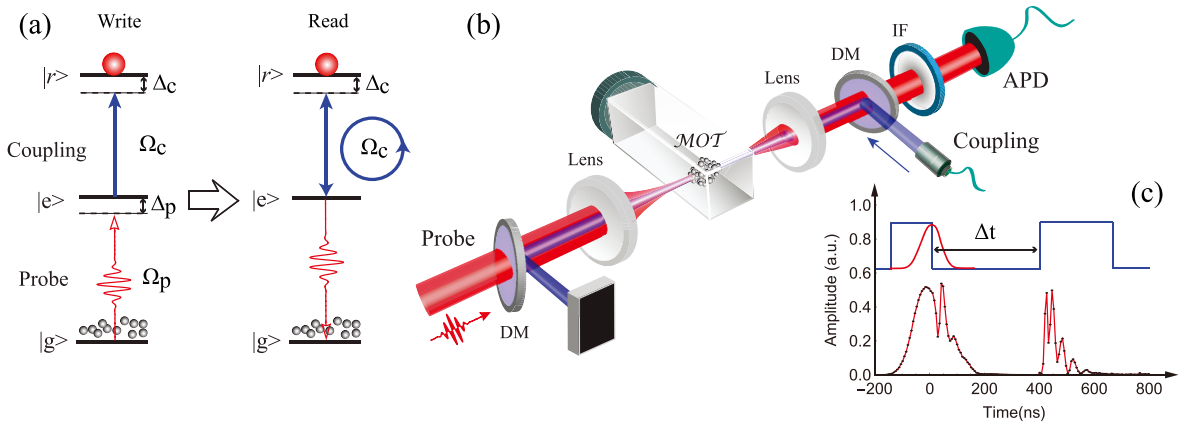

Fig. 1. Experimental setup and diagram. (a) Schematic of the energy diagram of write and read processes, the ladder-type atomic configuration with ground state $5S_{1/2}(F=3)$ ($|g\rangle$), excited state $5P_{3/2}(F'=4)$ ($|e\rangle$) with a linewidth of γ_e, and highly-excited state $|nD_{5/2}\rangle$ ($|r\rangle$) with a linewidth of γ_r. Ω_p and Ω_c are the corresponding Rabi frequencies of the probe and coupling fields. The probe (coupling) detuning are denoted by $\Delta_{p(c)}$. The wavelengths of the probe and coupling fields are 780 nm and 480 nm respectively. (b) Experimental setup of Rydberg quantum memory. (c) Time sequence for storage process. Δt represents the storage time. Labels: DM-dichroic mirror, IF-interference filter, APD single-photon detector, and MOT magneto-optic traps.

time sequence are shown in Figs. 1a–1c. The sample media is an optically thick atomic ensemble of Rubidium 85 trapped in MOT. This atomic cloud has a size of 500 μm with a temperature ~ 20 μK and an average density of ~ 1.0×10^{11} cm^{-3} at the center of the cloud. The optical depth (OD) in MOT is approximately 20. The probe field is then input into the atomic cloud using a beam waist ~5 μm in the center of the MOT estimated by fluorescence imaging, which is covered by the coupling beam with a beam waist of 16 μm. With a coupling laser beam, we demonstrate the quantum memory via Rydberg-EIT in the ladder-type atomic configuration, consisting of a ground state $|g\rangle$, an excited state $|e\rangle$, and a highly-excited Rydberg state $|r\rangle$; here, $n = 50$. The probe and coupling fields are counter-propagating, and couple the two-photon transitions $|g\rangle \rightarrow |e\rangle \rightarrow |r\rangle$, forming a Ladder-type EIT. The bandwidth of the transparency window of Rydberg-EIT is measured as $\delta w \sim 2\pi\times5$ MHz.

The probe field has a pulse width of 200 ns. The coupling field is modulated into double rectangular pulses with a width of 400 ns to demonstrate the write and read operations. The amplitudes and frequencies of the write and read pulses are tuned individually by an electro-optic modulator (EOM, LM 0202, Germany) and an acoustic-optic modulator (AOM) respectively; therefore, we can turn on/off the coupling field with fast rising and falling time. This guarantees that the probe is efficiently converted into the Rydberg polariton. We adiabatically switch off the coupling field, and a stored high-lying Rydberg-state super atom is obtained given by $1/\sqrt{N_m}\sum e^{i\mathbf{k}_S\cdot\mathbf{r}_i}|g\rangle_1\cdots|r\rangle_i\cdots|g\rangle_{N_m}$ [27–30], also referred to as a Rydberg polariton. $k_S = k_c - k_p$ is the wave vector of the atomic polariton, k_c and k_p are the vectors of the coupling and probe fields and $\mathbf{r}_i$ denotes the position of the i-th atom in atomic cloud. After a programmed storage time, the polariton is converted back into photonic excitation by switching on the coupling laser again. Fig. 1c shows the storage sequence for the probe pulse; the leaked and retrieved probe fields both exhibit oscillation.

The repetition rate of our experiment is 200 Hz, and the MOT trapping time is 4.71 ms. Moreover, the experimental window is 290 μs. The probe field is collected into a single-mode fiber and detected by a single-photon detector (avalanche diode, PerkinElmer SPCM-AQR-16-FC, 60% efficiency, maximum dark count rate of 25/s). The two detectors are gated by an arbitrary function generator. The signal from the single-photon detector and the triggered signal from the arbitrary function generator are then sent to a time-correlated single-photon counting system (TimeHarp 260) to measure the probe temporal profile.

3 Results

3.1 Theoretical analysis

In the storage process, the input probe field contains approximately 10 photons per pulse, and the efficiency of converting the photons to Rydberg polaritons is measured as ~ 0.04, guaranteeing one polariton excitation in the one storage process. The probe field illuminates the entire ensemble and excites all atoms with equal probability. Owing to the L-length cylinder mesoscopic atomic ensemble along the direction of probe beam, our system can be regarded as quasi-one-dimensional mesoscopic atomic ensemble, see the schematic diagram in Fig. 2a. After storing the probe pulse in this medium, the converted Rydberg polariton can be expressed as

$$|R_m\rangle = \frac{1}{\sqrt{\mathcal{N}_m}}\sum_{i=1}^{i=\mathcal{N}_m} e^{i\Delta\mathbf{k}\cdot\mathbf{r}_i}\left|g_1\cdots r_i\cdots g_{\mathcal{N}_m}\right\rangle \quad (1)$$

where $\mathcal{N}_m$ is the atom number in interacted area m, $\Delta\mathbf{k}$ is the wave-vector mismatch between the probes, and coupling fields, $\mathbf{r}_i$ is the position of atom i. Accordingly, the low-lying collective excited state is given

$$|E_m\rangle = \frac{1}{\sqrt{\mathcal{N}_m}}\sum_{i=1}^{i=\mathcal{N}_m} e^{i\mathbf{k}_p\cdot\mathbf{r}_i}\left|g_1\cdots e_i\cdots g_{\mathcal{N}_m}\right\rangle \quad (2)$$

Owing to the atoms loss and nonlinear conversion in the reading process, the size of the collective states $|E_m\rangle$ or $|R_m\rangle$ decreased. This reduction can be observed by observing the populations $|E_m\rangle$ or $|R_m\rangle$ under the driving of the coupling

DOI: 10.52396/JUSTC-2021-0239
JUSTC, 2022, 52(4): 1

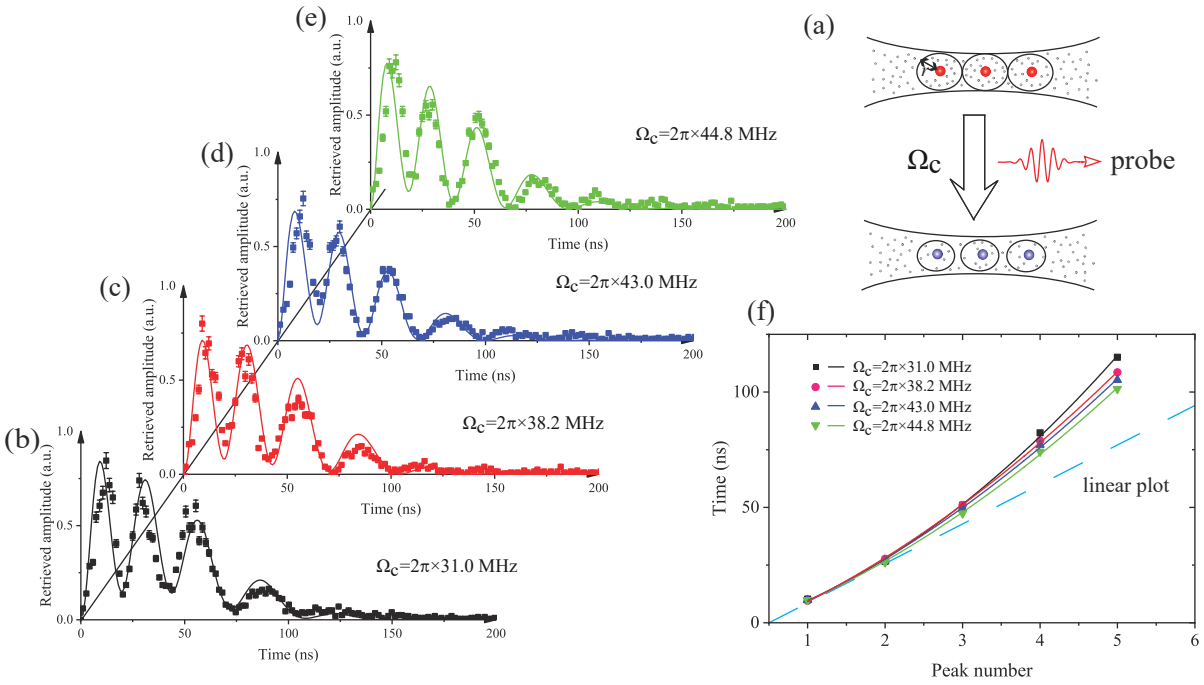

Fig. 2. Coherent retrieval signal with Rabi oscillations. (a) Schematic diagram of reading Rydberg polaritons out. The black sphere represents the ground-state atom, the red and blue spheres correspond to a high-lying Rydberg atom and low-lying excited atom. The size of the collective state is reduced as the number of atoms decreases. (b)–(e) The retrieved probe field versus time under different Ω_c; solid curves are fits of the form $P_s(\beta,C,t_0,\Omega_n,t)$, with different parameters: β, C, t_0, and Ω_n. (f) Measured time at different oscillation peaks. The data were fitted using the polynomial function $y=y_0+bx+cx^2$. The fitted parameters (y_0,b,c) are (–2.7,9.5,2.8) for the black data, (–6.0,13.2,1.9) for red data, (–5.1,12.6,1.92) for blue data and (–3.9,11.4,1.94) for green data. In this process, the detuning is $\Delta_p=-2\pi\times2.7$ MHz and $\Delta_c=2\pi\times14.8$ MHz for writing, and $\Delta_c=2\pi\times23.4$ MHz for reading. All error bars in the experimental data are estimated using Poisson statistics.

laser beam. The low-lying collective excited state is converted into the $\boldsymbol{k}_p$-photon pulse with an efficiency of η, $|E_m\rangle\rightarrow\sqrt{\eta}|G_m\rangle+\sqrt{1-\eta}|E_m\rangle$, here $|G_m\rangle=\left|g_1\cdots g_i\cdots g_{N_m}\right\rangle$ which is the ground state with multiple atoms. In this process, the loss of atoms is influenced by driving the coupling laser beam, in which there is no emitted probe field. The nonlinear converted efficiency η is dependent on the experimental parameters, such as OD, γ_e, Ω_c and Δ_c in the reading process, as the quantum memory is regarded as a delayed four-wave mixing process[22]. Consequently, the collective Rabi frequency coupling the collective state $|R_m\rangle$ and $|E_m\rangle$ becomes[31]

$$\begin{aligned}\Omega_{\rm coll}=&-\frac{e\varepsilon}{\hbar}\langle E_m|\boldsymbol{r}|R_m\rangle=\\&-\frac{e\varepsilon}{\hbar}\frac{\sqrt{\eta}}{\sqrt{N_m}}\sum_{i=1}^{i=N_{m'}}\langle g_1\cdots g_i\cdots g_{N_{m'}}|\mathbf{r}\left|g_1\cdots r_i\cdots g_{N_m}\right\rangle-\\&\frac{e\varepsilon}{\hbar}\frac{\sqrt{1-\eta}}{N_m}\sum_{i=1}^{i=N_{m'}}\langle g_1\cdots e_i\cdots g_{N_{m'}}|\mathbf{r}\left|g_1\cdots r_i\cdots g_{N_m}\right\rangle=\\&\frac{N_{m'}}{\sqrt{N_m}}\sqrt{\eta}\Omega_g+\frac{N_{m'}}{N_m}\sqrt{1-\eta}\Omega\end{aligned}\tag{3}$$

Here, $N_{m'}$ is the remaining number of ground state atoms owing to the loss induced by blue laser driving. $\Omega_g=-\frac{e\varepsilon}{\hbar}\langle g|\boldsymbol{r}|r\rangle$, corresponds to the Rabi frequency of a two-level single atom between the ground state $|g\rangle$ and Rydberg state $|r\rangle$ and $\Omega=-\frac{e\varepsilon}{\hbar}\langle e|\boldsymbol{r}|r\rangle$ corresponds to the Rabi frequency of a two-level single atom between the excited state $|e\rangle$ and Rydberg state $|r\rangle$. The first term corresponds to the enhanced effective Rabi frequency, which was not considered in our experiment (we detected only the transition process between $|e\rangle$ and $|r\rangle$). The Eq.(3) gives rise to an anomalous oscillation between the residual low-lying collective excited state $|E_m\rangle$ and the high-lying Rydberg-state super atom $|R_m\rangle$, with a decreased Rabi frequency $N_{m'}\Omega\sqrt{1-\eta}/N_m$. Because the quantum state $|E_m\rangle$ is continuously converted to $|G_m\rangle$ and the ground state atoms are lost during the reading process, the effective Rabi frequency $\Omega_{\rm coll}$ decreases with time during the oscillation as stated.

The reading process in our system can be modeled using a two-level atomic system with a varying effective Rabi frequency because the super atom could be regarded as a quasi-single particle. In the state evolution, as we consider the inhomogeneous broadening in our system, the broadening width can be embodied by the transparency bandwidth of the Rydberg-EIT. The probability of the retrieved signal is distributed as a Gaussian profile owing to the time reversal in the writing and reading processes[20, 32, 33] $\sim e^{-C^2t^2}$. The probability of the retrieved probe pulse under Rabi oscillation is expressed by[34]

$$\begin{aligned}&P_r(\beta,\Delta,C,t_0,\Omega_n,t)=\\&e^{-\beta^2(t-t_0)^2}\left(1-\cos\left(\sqrt{\frac{e^{-C^2t^2}+1}{2}}\Omega t\right)\right)\end{aligned}\tag{4}$$

The term $e^{-\beta^2(t-t_0)^2}$ is the fitted emission rate from a low-lying collective excited state to a photon; C^2 is the chirped coefficient, and t_0 is a parameter that fits the temporal profile of the probe intensity. The Rabi frequency $\Omega=\sqrt{\Delta^2+\Omega_n^2}$. Ω_n is

DOI: 10.52396/JUSTC-2021-0239
JUSTC, 2022, 52(4): 1

the effective Rabi frequency of the atomic transitions $|r\rangle$ and $|e\rangle$ involving Ω_c and Δ_c. The temporal profile of the retrieved probe field can be simulated by integrating the inhomogeneous shift Δ:

$$P_s(\beta,C,t_0,\Omega_n,t) = \int_{-\infty}^{+\infty} \sqrt{\pi/\alpha}\mathrm{e}^{-\alpha\Delta^2} P(\beta,\Delta,C,t_0,\Omega_n,t)\mathrm{d}\Delta \quad (5)$$

Here, we consider the energy broadening effect, which is distributed with a Gaussian function $\sqrt{\pi/\alpha}\mathrm{e}^{-\alpha\Delta^2}$; α is the broadening coefficient.

3.2 Size-reduction of Rabi oscillations

To explore the chirped character of the observed Rabi oscillations, we measure the temporal profile of the retrieved probe field with varying Ω_c. Here, we set $\Delta_p = -2\pi\times2.7$ MHz and $\Delta_c = 2\pi\times14.79$ MHz to write the Rydberg polariton and set $\Delta_c = 2\pi\times23.4$ MHz to read the Rydberg polariton out. We record the retrieved probe field, and deduce that the oscillation exhibits a period of gradual increase, which corresponds to a chirped pulse; the results are shown in Figs. 2b—2e. The effective Rabi frequency, Ω_n, was fitted as $2\pi\times46.1$ MHz, $2\pi\times47.7$ MHz, $2\pi\times49.3$ MHz, and $2\pi\times50.9$ MHz, as shown in Figs. 2b—2e, which tend to be consistent with Ω_n^{exp} at large Ω_c by considering the effective Rabi frequency $\Omega_n^{exp} = \sqrt{\Omega_c^2+\Delta_c^2}$. The different peaks against time are plotted in Fig. 2f, which are fitted by the polynomial function $y = y_0 + bx + cx^2$ different from the normal fixed oscillation period with linear behavior. The collective state $|E_m\rangle$ is continuously converted to $|G_m\rangle$ during the reading process and the collective Rabi frequency gradually decreased over time. This observation differs from previous works[6]. The Rabi oscillation is demonstrated with fixed N_m and Ω, thus the Rabi frequency is a constant of $\sqrt{N_m}\Omega$.

This process can be regarded as shaping a light pulse; the advantage of shaping a light pulse with this method is that the shaping operation is on-demand. Next, we change the storage time Δt and record the retrieved probe field; the results are shown in Figs. 3b— 3e. Dephasing also occurs during the storage process, which affects the coherence of the Rabi oscillations between the collective $|R_m\rangle$ and $|E_m\rangle$. In the Bloch sphere given in Fig. 3a, the trajectory of rotations driven by the coupling field do not express a curve but a surface because the point on the Bloch sphere is replaced by a sphere surface. The size of the sphere surface is determined by the broadening coefficient α. The broadening effect reduces the visibility of the Rabi oscillations and may even suppress them significantly as decoherence in the storage process[35, 36]. As observed in Fig. 3b, the retrieved probe pulse shows an obviously decreased visibility which is marked by the red arrow. When increasing the storage time from $\Delta t = 200$ ns to $\Delta t = 500$ ns, the visibility is further reduced, as shown in Figs. 3b— 3e because of the increased α. This is because the collective state is dephased during storage, which generates a finite storage lifetime. The atoms in the MOT are not spin-polarized, and the absence of spin polarization with respect to light leads to an inhomogeneous broadening of the Rabi fre-

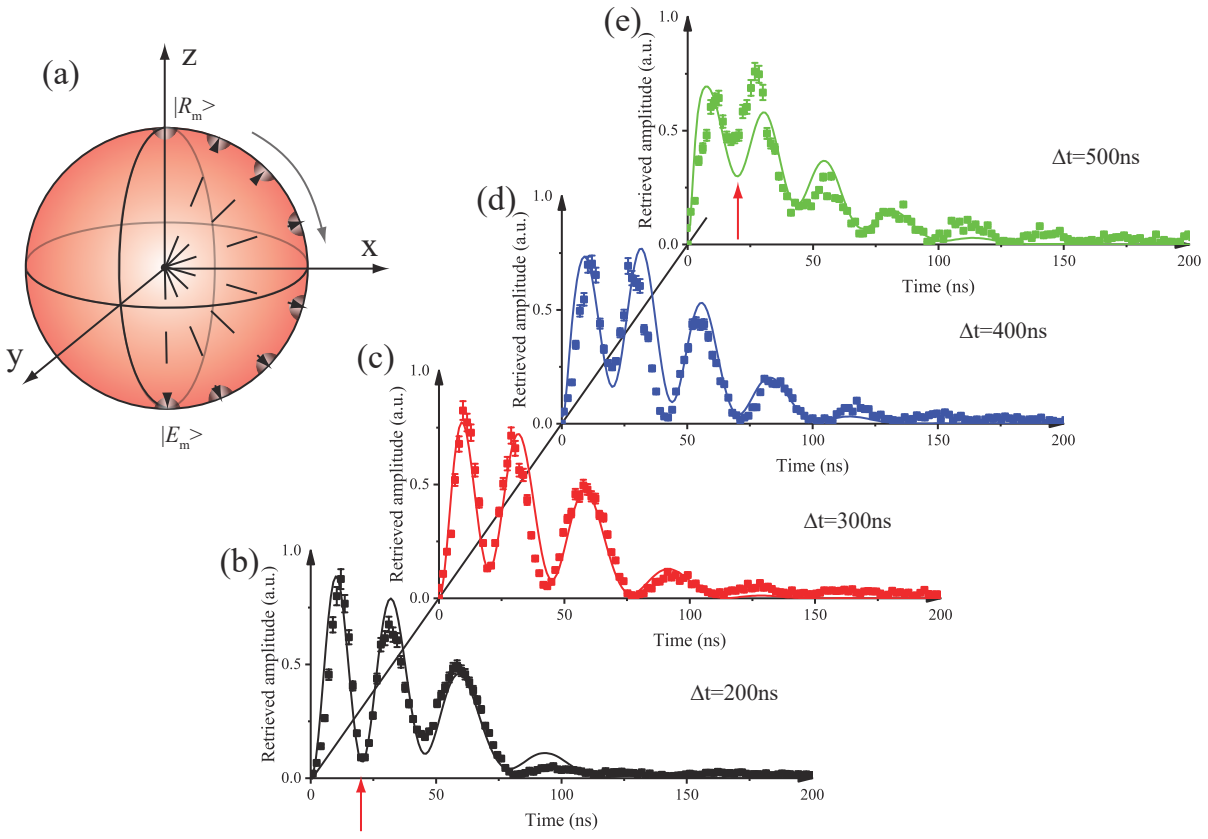

Fig. 3. Measurement of retrieved probe field. (a) Bloch sphere for Rabi oscillation with inhomogeneous broadening. (b-e), the retrieved probe field against time under different storage times Δt; The solid curves are fits of the form $P_s(\beta,C,t_0,\Omega_n,t)$. In this process, the detunings $\Delta_p = -2\pi\times2.7$ MHz and $\Delta_c = 2\pi\times14.8$ MHz for writing, and $\Delta_c = 2\pi\times17.6$ MHz for reading. All error bars in the experimental data are estimated from the Poisson statistics.

DOI: 10.52396/JUSTC-2021-0239
JUSTC, **2022**, 52(4): 1

quencies and, therefore, to dephasing. Additionally, the inhomogeneous Ω_c caused by the transverse differentiated intensity distribution of the coupling field induce additional dephasing. The broadening effect reflects the broadened bandwidth of the transparency window of the Rydberg EIT, as given in Ref. [37].

Moreover, we changed the detuning Δ_c to explore the evolution of the collective state. In this process, we write the high-lying Rydberg-state super atom under the optimized condition $\Delta_p = -2\pi\times 2.7$ MHz and $\Delta_c = 2\pi\times 14.8$ MHz. In the read process, the temporal profile of the retrieved probe field is changed by varying Δ_c. The results are given in Figs. 4a—4e, in which the detuning Δ_c is changed to $-2\pi\times 12$ MHz (Fig. 4a), $2\pi\times 17.6$ MHz (Fig. 4b), and $2\pi\times 26$ MHz (Fig. 4c) respectively. The periods of these oscillations are clearly increased as the effective Rabi frequencies are increased versus Δ_c. The theoretical function fits the results in Fig. 4b and Fig. 4c but with uncertainty deviations for the red detuning of Δ_c as shown in the example in Fig. 4a.

When the detuning Δ_c is large enough, we can evaluate more complex oscillations shown in Figs. 4e— 4f. In these two cases, we set the detuning $\Delta_c = 2\pi\times 35$ MHz and $\Delta_c = 2\pi\times 44$ MHz, respectively. The constructive and destructive interference appeared alternately along the time axis in Figs. 4e and 4f supports a superposition of two Rabi oscillations, with fitted Rabi frequencies $\Omega_n = 2\pi\times 41.4$, $2\pi\times$ 62.1 MHz for Fig. 4e and $\Omega_n = 2\pi\times 49.3$, $2\pi\times 68.4$ MHz for Fig. 4f. Accordingly, the system is described by state $|\psi\rangle = c_1|R_{m1}\rangle + c_2|R_{m2}\rangle + c_3|E_m\rangle$. The coefficients c_1, c_2 and c_3 are the time-dependent complex amplitudes, here $|R_{m1}\rangle$ and $|R_{m2}\rangle$ correspond to the states of high-lying Rydberg-state super atoms. However, for the red detuning $\Delta_c = -2\pi\times 35$ MHz in Fig. 4d completely opposite to the case in Fig. 4e, there is a single oscillation with fitted Rabi frequencies $\Omega_n = 2\pi\times 41.4$ MHz. The measured data with $\Delta_c = \pm 2\pi\times 35$ MHz with asymmetric Rabi oscillations supports that an enhanced Rabi oscillation process occurs under blue detuning.

4 Conclusions

In summary, the entire process of the Rydberg-quantum memory with Rabi oscillation can be considered as manipulating a Rydberg super atom to shape the photon wave-packet. The unique technology to modulate the photon wave-packet presented here is based on the Rabi oscillation between different collective excited states. This is significantly different from the progresses of using electro-optical modulators to directly modulate the amplitude of single-photon wave packets[38, 39] or modulating the properties of pump fields by electro-optical modulators and spatial light modulation to change the temporal quantum waveform of narrowband biphotons in cold atoms[40, 41], or modulating photonic bandwidth through sum frequency generation[42, 43]. The anomalous Rabi oscillations hint that the arbitrary photonic wave-packet could be constructed via superposing multi-polaritons with more tunable detunings. The reported results combined the techniques of quantum memory and the anomalous Rabi oscillations have potential in modulating the single photon wave-packet[21] and provide a perspective approach of constructing an interface between light and the atoms to study collective effect. Additionally, this can be regarded as a tool to realize the manipulation of the quantum state towards the study of quantum mechanics in the microscopic field.

Acknowledgements

The authors would like to thank Prof. Wei Zhang, Jinming Cui, and Prof. Xiangdong Chen for the initial discussions on the results, Prof. Lin Li from Huazhong University of Science and Technology and Prof. Yuan Sun from the National University of Defense Technology for their valued discussions. This work was supported by the National Key R&D Program of China (2017YFA0304800), the National Natural Science Foundation of China (U20A20218, 61525504, 61435011), Fundamental Research Funds for the Central Universities, and the Youth Innovation Promotion Association of CAS(2018490).

Conflict of interest

The authors declare that they have no conflict of interest.

Biographies

Dongsheng Ding is a Professor at the University of Science and Tech-

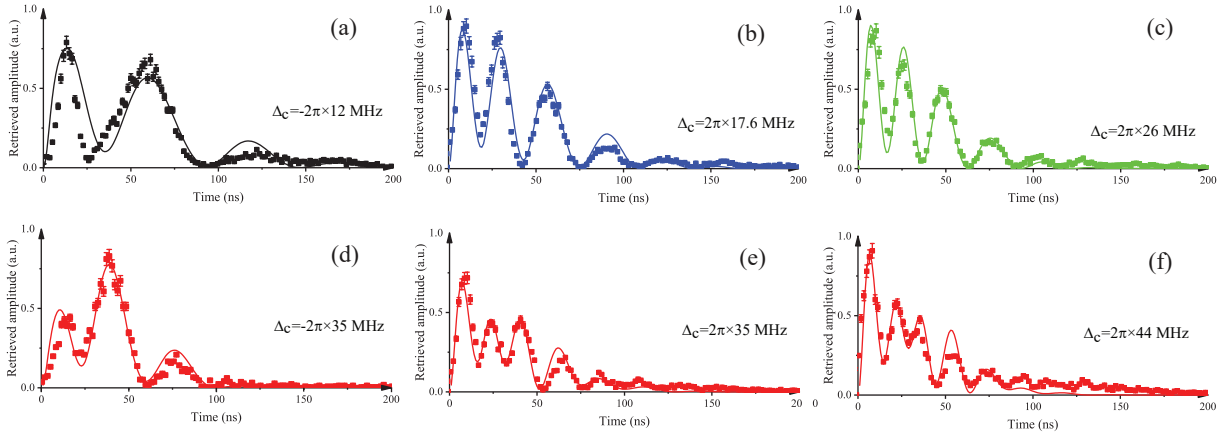

Fig. 4. Measurement of retrieved probe field with different detuning Δ_c. (a) to (e) Retrieved probe field against detuning Δ_c; solid curves are fits of the form $P_s(\beta, C, t_0, \Omega_n, t)$ with the fit parameters $(\beta, C, t_0, \Omega_n)$. In this process, the storage time was set to 300 ns and $\Omega_c = 2\pi\times 44.8$ MHz. All error bars in the experimental data are estimated using Poisson statistics.

DOI: 10.52396/JUSTC-2021-0239
JUSTC, **2022**, 52(4): 1

nology of China (USTC). His recent interest fields are quantum simulation, quantum metrology by Rydberg atoms. He received his PhD degree from USTC in 2015. He has published more than 80 papers in international high-level journals including *Sci. Adv., Nat. Photo., Nat. Comm., PRL, PRX, Light Sci. and App.*, and has obtained a series of original achievements.

Yichen Yu is a PhD graduate at the University of Science and Technology of China. His research field is light and atoms interaction.

Baosen Shi is a Professor at the University of Science and Technology of China (USTC). His research field is light and matter interaction. He received his PhD degree from USTC in 1998. He has published more than 100 papers in international high-level journals including *Sci. Adv., Nat. Photo., Nat. Comm., PRL, PRX, Light Sci. and App.*, and has obtained a series of original achievements.

References

[1] Guerin W, Rouabah M T, Kaiser R. Light interacting with atomic ensembles: Collective, cooperative and mesoscopic effects. *Journal of Modern Optics,* **2017**, *64*: 895–907.

[2] Dicke R H. Coherence in spontaneous radiation processes. *Physical Review,* **1954**, *93*: 99–110.

[3] Honer J, Löw R, Weimer H, et al. Artificial atoms can do more than atoms: Deterministic single photon subtraction from arbitrary light fields. *Physical Review Letters,* **2011**, *107*: 093601.

[4] Gaëtan A, Miroshnychenko Y, Wilk T, et al. Observation of collective excitation of two individual atoms in the Rydberg blockade regime. *Nature Physics,* **2009**, *5*: 115–118.

[5] Urban E, Johnson T A, Henage T, et al. Observation of Rydberg blockade between two atoms. *Nature Physics,* **2009**, *5*: 110–114.

[6] Dudin Y O, Li L, Bariani F, et al. Observation of coherent many-body Rabi oscillations. *Nature Physics,* **2012**, *8*: 790–794.

[7] Zeiher J, Schauß P, Hild S, et al. Microscopic characterization of scalable coherent Rydberg superatoms. *Physical Review X,* **2015**, *5*: 031015.

[8] Weber T M, Höning M, Niederprüm T, et al. Mesoscopic Rydberg-blockaded ensembles in the superatom regime and beyond. *Nature Physics,* **2015**, *11*: 157–161.

[9] Beterov I I, Saffman M, Yakshina E A, et al. Simulated quantum process tomography of quantum gates with Rydberg superatoms. *Journal of Physics B:Atomic, Molecular and Optical Physics,* **2016**, *49*: 114007.

[10] Paris-Mandoki A, Braun C, Kumlin J, et al. Free space quantum electrodynamics with a single Rydberg superatom. *Physical Review X,* **2017**, *7*: 041010.

[11] Busche H, Huillery P, Ball S W, et al. Contactless nonlinear optics mediated by long-range Rydberg interactions. *Nature Physics,* **2017**, *13*: 655–658.

[12] Lukin M D, Fleischhauer M, Cote R, et al. Dipole blockade and quantum information processing in mesoscopic atomic ensembles. *Phys. Rev. Lett.,* **2001**, *87*: 037901.

[13] Saffman M. Quantum computing with atomic qubits and Rydberg interactions: Progress and challenges. *Journal of Physics B:Atomic, Molecular and Optical Physics,* **2016**, *49*: 202001.

[14] Firstenberg O, Adams C S, Hofferberth S. Nonlinear quantum optics mediated by Rydberg interactions. *Journal of Physics B:Atomic, Molecular and Optical Physics,* **2016**, *49*: 152003.

[15] Schauß P, Cheneau M, Endres M, et al. Observation of spatially ordered structures in a two-dimensional Rydberg gas. *Nature,* **2012**, *491*: 87–91.

[16] Labuhn H, Barredo D, Ravets S, et al. Tunable two-dimensional arrays of single Rydberg atoms for realizing quantum Ising models. *Nature,* **2016**, *534*: 667–680.

[17] Ding D S, Busche H, Shi B S, et al. Phase diagram and self-organizing dynamics in a thermal ensemble of strongly interacting Rydberg atoms. *Physical Review X,* **2020**, *10*: 021023.

[18] Ding D S, Liu Z K, Busche H, et al. Epidemic spreading and herd immunity in a driven non-equilibrium system of strongly-interacting atoms. https://arxiv.org/abs/2106.12290.

[19] Bussières F, Sangouard N, Afzelius M, et al. Prospective applications of optical quantum memories. *Journal of Modern Optics,* **2013**, *60*: 1519–1537.

[20] Ding D S, Wang K, Zhang W, et al. Entanglement between low and high-lying atomic spin waves. *Phys. Rev. A,* **2016**, *94*: 052326.

[21] Dudin Y O, Kuzmich A. Strongly interacting Rydberg excitations of a cold atomic gas. *Science,* **2012**, *336*: 887–889.

[22] Ripka F, Kübler H, Löw R, et al. A room-temperature single-photon source based on strongly interacting Rydberg atoms. *Science,* **2018**, *362*: 446–449.

[23] Du S, Wen J, Rubin M H. Narrowband biphoton generation near atomic resonance. *JOSA B,* **2008**, *25*: C98–C108.

[24] Mendes M S, Saldanha P L, Tabosa J W R, et al. Dynamics of the reading process of a quantum memory. *New Journal of Physics,* **2013**, *15*: 075030.

[25] De Oliveira R A, Mendes M S, Martins W S, et al. Single-photon superradiance in cold atoms. *Physical Review A,* **2014**, *90*: 023848.

[26] Saffman M, Walker T G, Mølmer K. Quantum information with Rydberg atoms. *Reviews of Modern Physics,* **2010**, *82*: 2313–2363.

[27] Fleischhauer M, Imamoglu A, Marangos J P. Electromagnetically induced transparency: Optics in coherent media. *Reviews of Modern Physics,* **2005**, *77*: 633–673.

[28] Ding D S, Zhou Z Y, Shi B S, et al. Single-photon-level quantum image memory based on cold atomic ensembles. *Nature Communications,* **2013**, *4*: 2527.

[29] Ding D S, Jiang Y K, Zhang W, et al. Optical precursor with four-wave mixing and storage based on a cold-atom ensemble. *Physical Review Letters,* **2015**, *114*: 093601.

[30] Ding D S, Zhang W, Zhou Z Y, et al. Raman quantum memory of photonic polarized entanglement. *Nature Photonics,* **2015**, *9*: 332–338.

[31] Tresp C. Rydberg polaritons and Rydberg superatoms: Novel tools for quantum nonlinear optics. Stuttgart, Germany: University of Stuttgart, 2017.

[32] Novikova I, Gorshkov A V, Phillips D F, et al. Optimal control of light pulse storage and retrieval. *Physical Review Letters,* **2007**, *98*: 243602.

[33] Everett J L, Vernaz-Gris P, Campbell G T, et al. Time-reversed and coherently enhanced memory: A single-mode quantum atom-optic memory without a cavity. *Physical Review A,* **2018**, *98*: 063846.

[34] Stanojevic J, Côté R. Many-body Rabi oscillations of Rydberg excitation in small mesoscopic samples. *Physical Review A,* **2009**, *80*: 033418.

[35] De Léséleuc S, Barredo D, Lienhard V, et al. Analysis of imperfections in the coherent optical excitation of single atoms to Rydberg states. *Physical Review A,* **2018**, *97*: 053803.

[36] Levine H, Keesling A, Omran A, et al. High-fidelity control and entanglement of Rydberg-atom qubits. *Physical Review Letters,* **2018**, *121*: 123603.

[37] Yu Y C, Dong M X, Ye Y H, et al. Experimental demonstration of switching entangled photons based on the Rydberg blockade effect. *Science China:Physics, Mechanics & Astronomy,* **2020**, *63*: 110312.

[38] Kolchin P, Belthangady C, Du S, et al. Electro-optic modulation of single photons. *Physical Review Letters,* **2008**, *101*: 103601.

[39] Specht H P, Bochmann J, Mücke M, et al. Phase shaping of single-photon wave packets. *Nature Photonics,* **2009**, *3*: 469–472.

[40] Chen J F, Zhang S, Yan H, et al. Shaping biphoton temporal waveforms with modulated classical fields. *Physical Review Letters,* **2010**, *104*: 183604.

[41] Zhao L, Guo X, Sun Y, et al. Shaping the biphoton temporal waveform with spatial light modulation. *Physical Review Letters,* **2015**, *115*: 193601.

[42] Rakher M T, Ma L, Davan M, et al. Simultaneous wavelength translation and amplitude modulation of single photons from a quantum dot. *Physical Review Letters,* **2011**, *107*: 083602.

[43] Lavoie J, Donohue J M, Wright L G, et al. Spectral compression of single photons. *Nature Photonics,* **2013**, *7*: 363–366.

DOI: 10.52396/JUSTC-2021-0239
JUSTC, **2022**, 52(4): 1